JETIR.ORG ISSN: 2349-5162 | ESTD Year : 2014 | Monthly Issue
JOURNAL OF EMERGING TECHNOLOGIES AND INNOVATIVE RESEARCH (JETIR)
An International Scholarly Open Access, Peer-reviewed, Refereed Journal

COMPUTATIONAL SCREENING OF *Saraca asoca* PHYTOCHEMICALS AGAINST THYMIDINE KINASE AND TYPE II PROTEASE OF HERPES VIRUS

Shivam Mishra[1], Prabhat Kumar[2], Nidhi Mishra[3]

[1, 2]School of Life sciences, Singhania university, Pacher Bari, Rajasthan, India

[3] Department of Applied Sciences, Indian Institute of Information Technology, Jhalwa, Prayagraj

Abstract

Herpesviruses are a major global health concern, requiring the development of novel antiviral therapeutics. In this study, we explored the potential of leucocianidol, a bioactive flavonoid from *Saraca asoca*, as an inhibitor of thymidine kinase (TK) and type II protease, two essential enzymes for herpesvirus replication. Molecular docking analysis revealed strong binding affinities of leucocianidol towards these targets, suggesting its potential inhibitory activity. ADME (Absorption, Distribution, Metabolism, and Excretion) and toxicity evaluations demonstrated favorable pharmacokinetic properties, including high gastrointestinal absorption, optimal distribution, and minimal toxicity risks. Density Functional Theory (DFT) calculations provided insights into the electronic properties and structural stability of leucocianidol, further supporting its reactivity and potential bioactivity. Molecular dynamics (MD) simulations were conducted to assess the stability of leucocianidol-TK and leucocianidol-protease complexes under physiological conditions, revealing stable interactions and minimal conformational fluctuations throughout the simulation period. The combined findings from molecular docking, ADME, toxicity assessment, DFT, and MD simulations suggest that leucocianidol could serve as a promising lead compound for anti-herpetic drug development. However, further in vitro and in vivo studies are required to validate its efficacy and safety. This study underscores the significance of computational approaches in drug discovery and highlights the antiviral potential of natural compounds.

Keywords: *Saraca asoca*, leucocianidol, herpesvirus, thymidine kinase, type II protease

Introduction

Herpesviruses, including herpes simplex virus (HSV), varicella-zoster virus (VZV), cytomegalovirus (CMV), and Epstein-Barr virus (EBV), cause diverse diseases and establish lifelong latency, reactivating under immunosuppression (Mettenleiter et al., 2019). Current antivirals like acyclovir target viral DNA polymerase but face challenges from drug resistance and limited efficacy against latent infections (Das & Hong, 2019). Thymidine kinase (TK) and type II protease, critical for viral replication and protein processing, are promising targets for novel therapies (Xie et al., 2019; Sharma & Gupta, 2017).

Natural compounds, particularly flavonoids, offer potential antiviral properties with low toxicity (Mishra et al., 2025). Leucocianidol, a flavonoid from *Saraca asoca* (Ashoka tree), exhibits pharmacological activities but its interactions with TK and type II protease remain unexplored (Rathod & Ghante, 2021). In silico methods, including molecular docking, ADME-toxicity analysis, DFT calculations, and molecular dynamics (MD) simulations, enable efficient evaluation of drug candidates (Panigrahi & Sahu, 2025).

This study investigates leucocianidol's potential as an inhibitor of TK and type II protease using computational approaches. Molecular docking assesses binding affinities, ADME-toxicity evaluates pharmacokinetics, DFT examines electronic properties, and MD simulations confirm complex stability. These findings aim to advance leucocianidol as a lead compound for anti-herpetic drug development, addressing drug-resistant herpesviruses (Treml et al., 2020).

Methodology:

Data Retrieval

Phytochemicals from *Saraca asoca* were retrieved in mol2 format from the IMPPAT database, a repository of Indian medicinal plants and phytochemicals (Vivek-Ananth et al., 2023). Target proteins, type II protease (PDB-ID: 1AT3, 2.50 Å resolution) and thymidine kinase (PDB-ID: 1KI3, 2.37 Å resolution) from HSV-1, were obtained in .pdb format from the Protein Data Bank (Hoog et al., 1997; Champness et al., 1998). High-resolution structures ensured reliable molecular docking and simulation studies.

Protein and Ligand Preparation

Proteins type II protease (PDB-ID: 1AT3) and thymidine kinase (PDB-ID: 1KI3) were prepared using AutoDock 1.5.7 (Morris et al., 2009). Water molecules, heteroatoms, and non-essential ligands were removed, polar hydrogens added, and Kollman charges assigned (Bayly et al., 1993). Proteins were saved in pdbqt format. Ligands from IMPPAT (mol2 format) were processed with AutoDock Tools, adding Gasteiger charges, merging non-polar hydrogens, and defining rotatable bonds, then saved as pdbqt (Trott & Olson, 2010). Grid boxes encapsulated active sites: for 1AT3, spacing 0.675 Å, dimensions x=62, y=74, z=118, center x=26.698, y=23.339, z=23.785; for 1KI3, spacing 0.547 Å, dimensions x=112, y=114, z=108, center x=32.053, y=83.144, z=45.180.

Molecular Docking

Molecular docking was performed using AutoDock Vina to assess binding of *Saraca asoca* phytochemicals with type II protease (PDB ID: 1AT3) and thymidine kinase (PDB ID: 1KI3). Prepared pdbqt files were docked within predefined grid boxes with an exhaustiveness value of 8. Best conformations, selected by lowest binding energy and hydrogen bonds, were analyzed using Chimera and Discovery Studio for molecular interactions.

ADME Analysis

Leucocianidol's pharmacokinetic properties and drug-likeness were evaluated using SwissADME (Daina et al., 2017). The compound's SMILES notation was input to predict parameters like lipophilicity, solubility, and bioavailability, and compliance with Lipinski, Ghose, Veber, and Egan rules. The results informed leucocianidol's absorption, distribution, metabolism, and excretion profile for therapeutic development.

Toxicity Analysis

Leucocianidol's toxicity was assessed using Protox-3 (Banerjee et al., 2018). Its SMILES notation was input to predict toxicity class, LD_{50}, hepatotoxicity, carcinogenicity, immunotoxicity, mutagenicity, and cytotoxicity, evaluating its safety for therapeutic use.

DFT Analysis

Leucocianidol and its complexes with 1AT3 and 1KI3 were analyzed using DFT to assess electronic properties and stability. Avogadro (Hanwell et al., 2012) generated input files, MOPAC (Stewart, 2016) computed HOMO-LUMO gap, total energy, and molecular orbitals, and Jmol (Hanson, 2010) visualized electronic behavior and reactivity.

Molecular Dynamics Simulation

MD simulations using GROMACS 2022.6 (Abraham et al., 2015) assessed stability and dynamics of apoproteins (1AT3, 1KI3), leucocianidol, and valacyclovir complexes. Structures in .pdb format were parameterized with CHARMM force field (Vanommeslaeghe et al., 2010), solvated in TIP3P water (Jorgensen et al., 1983), and neutralized with 0.15 M NaCl. Systems underwent energy minimization, NVT/NPT equilibration (100 ps each), and 100 ns production runs at 300 K, 1 bar. Analyses included RMSD, RMSF, radius of gyration, H-bonds, DSSP secondary structure, SASA, PCA, and FEL to evaluate stability, flexibility, and binding. Leucocianidol complexes were compared with valacyclovir and apoproteins to assess inhibitory potential.

Result & Discussion

Molecular Docking Analysis

Molecular Docking studies revealed binding energies of phytochemicals with Type II Protease (1AT3) and Thymidine Kinase (1KI3) (Table 1). Valacyclovir bound to 1AT3 with binding energy -5.3 kcal/mol, and interacted with residues LEU:223, ASP:225, TRP:227, ARG226, ASN:220, MET:221, ALA:217 of chain B and ALA:217, TYR:124, THR:216, ALA:153, ASN:220, MET:221, ARG:226 of chain A (Fig1A,I), and to 1KI3 with binding energy of -5.0 kcal/mol, and interacted with residues SER:321, LYS:317, ARG:318, THR:197, PRO:196, of chain A and amino acids PRO:141, ALA:137, PRO:196, ALA:140, LEU:198 of chain B (Fig1A, III). Leucocianidol showed the highest affinity: -9.7 kcal/mol with 1AT3, and interacted with residues LEU: 223, ARG:224, ASP:225, TRP:227, ARG:226, ALA:217, MET:221, ASN:220, ALA:153, THR:216, TYR:124, ALA:127, of chain A and MET:221, ASN:220, ARG:226, LEU223, ASP:225 of chain B (Fig1A, II), and binding energy -8.6 kcal/mol with 1KI3, and interacted with residues ALA:186, THR:122, THR:183, VAL:119, ALA:118, GLN:185, of chain A and amino acids ILE:126, SER:123, ALA:124, ASN:99, THR:96GLU:95, SER:94, ALA:93, THR:127, GLY:92, TYR:87 of chain B. (Fig1A, IV). Leucocianidol shows strong inhibition of Type II Protease and Thymidine Kinase, with lower binding energy than valacyclovir. *Saraca asoca* phytochemicals, particularly leucocianidol, are promising antiviral agents against herpes virus. Molecular dynamics and in vitro studies are recommended for validation.

Table1: Binding affinities (ΔG) and inhibition constant (Ki) of Phytochemicals from *Sarasa asoca*, and reference molecules against Herpes Virus targets.

Se. No.	Phytochemicals	1AT3		1KI3	
		Binding Energy (Kcal/mol)	Inhibition Constant µM	Binding Energy (Kcal/mol)	Inhibition Constant µM
1.	beta-Sitosterol	-6.2	28.5	-6.5	17.18
2.	Catechol	-5.4	109.99	-5.5	92.91
3.	Cianidanol	-6.4	20.34	-7.5	3.18
4.	Epicatechin	-6.7	12.26	-6.8	10.35
5.	Ergometrine	-6.9	8.74	-7.6	2.68
6.	Myristic acid	-5.7	66.29	-3.9	1383.52
7.	Catechol	-5.3	130.22	-4.8	302.84
8.	Kaempferol 3-O-beta-D-glucoside	-7.4	3.76	-7.5	3.18
9.	Stearic acid	-4.3	704.29	-3.9	1383.52
10.	1-Octacosanol	-4	1168.63	-4	1168.63
11.	1-Hexacosanol	-3.4	3217.56	-4.2	833.8
12.	Palmitic acid	-4.3	704.29	-4.2	833.8
13.	Arachidic acid	-3.9	1383.52	-4.2	833.8
14.	leuco-cyanidin	-9.6	0.0917	-8.6	0.5
15.	Oleic acid	-3.8	1637.93	-4.5	502.5
16.	Gallic acid	-6.9	8.74	-5.3	130.22
17.	beta-Amyrin	-7.2	5.27	-7.9	1.62
18.	Clionasterol	-7	7.39	-6.3	24.08
19.	Cyanin	-7.6	2.68	-7.9	1.62
20.	Cosmosiin	-7.4	3.76	-8.2	0.97
21.	Isoquercitrin	-7.2	5.27	-7.4	3.76
22.	Linolenic acid	-6.4	20.34	-4.7	358.53
23.	Quercetin-3-glucoside	-7.7	2.27	-8.3	0.82
24.	beta-Sitosterol	-6.4	20.34	-6.9	8.74
25.	Epicatechin	-6.7	12.26	-7.2	5.27
26.	Linoleic acid	-6.4	20.34	-5	216.07
27.	Quercitrin	-7.4	3.76	-7.7	2.27
28.	Leucocianidol	-9.7	0.0775	-8.6	0.5
29.	Leucopelargonidin	-6.7	12.26	-7.2	5.27
30.	Octacosanol	-4.6	424.45	-3.4	3217.56
31.	Procyanidin	-7.9	1.62	-8.8	0.35
32.	Stigmast-5-en-3-ol	-6.2	28.5	-6.3	24.08
33.	Tannic acid	-7.2	5.27	-9.0	0.25
34.	Valacyclovir	-5.3	130.22	-5	216.07

ADME Analysis

Valacyclovir and leucocianidol showed suitable molecular weights and TPSA, with valacyclovir's higher TPSA suggesting lower permeability (Table 2, Fig1B). Leucocianidol had high GI absorption, unlike valacyclovir's low absorption. Neither crossed the blood-brain barrier nor inhibited CYP enzymes. Valacyclovir was a P-gp substrate. Both met Lipinski's Rule, but leucocianidol violated one hydrogen bond donor limit and triggered a catechol alert. Valacyclovir failed Veber/Ghose filters. Both had a 0.55 bioavailability score.

Table2: ADME analysis of Valacyclovir and Leucocianidol

Serial No.	Parameter	Leucocianidol	Valacyclovir
1.	Formula	C15H14O7	C13H20N6O4
2.	Molecular weight	306.27 g/mol	324.34 g/mol
3.	Molar Refractivity	75.50	82.54
4.	TPSA	130.61 Å²	151.14 Å²
5.	Log Po/w (iLOGP)	1.04	0.97
6.	Log S (ESOL)	-1.60	-1.23
7.	Class	Very soluble	Very soluble
8.	GI absorption	High	Low
9.	BBB permeant	No	No
10.	P-gp substrate	No	Yes

11.	Log Kp (skin permeation)	-8.70 cm/s	-8.71 cm/s
12.	Lipinski	Yes; 1 violation: NHorOH>5	Yes; 0 violation
13.	Ghose	Yes	No; 1 violation: WLOGP<-0.4
14.	Veber	Yes	No; 1 violation: TPSA>140
15.	Egan	Yes	No; 1 violation: TPSA>131.6
16.	Muegge	No; 1 violation: H-don>5	No; 1 violation: TPSA>150
17.	Bioavailability Score	0.55	0.55

Toxicity

Leucocianidol showed no organ toxicity (hepatotoxicity, neurotoxicity, cardiotoxicity), mutagenicity, cytotoxicity, ecotoxicity, or clinical toxicity (Table 3, Fig1 C). It did not affect nuclear receptor signalling, stress response pathways, or neurotransmitter receptors, nor inhibit CYP enzymes, suggesting minimal metabolic interference. These findings support leucocianidol's safety as a therapeutic candidate, but in vivo and clinical studies are needed for validation.

Table3: Toxicity analysis of Leucocianidol

Se. No.	Classification	Target	Shorthand	Prediction	Probability
1.	Organ toxicity	Hepatotoxicity	dili	Inactive	0.71
2.	Organ toxicity	Neurotoxicity	neuro	Inactive	0.91
3.	Organ toxicity	Cardiotoxicity	cardio	Inactive	0.95
4.	Toxicity end points	Mutagenicity	mutagen	Inactive	0.52
5.	Toxicity end points	Cytotoxicity	cyto	Inactive	0.95
6.	Toxicity end points	Ecotoxicity	eco	Inactive	0.52
7.	Toxicity end points	Clinical toxicity	clinical	Inactive	0.56
8.	Tox21-Nuclear receptor signalling pathways	Androgen Receptor (AR)	nr_ar	Inactive	0.99
9.	Tox21-Nuclear receptor signalling pathways	Androgen Receptor Ligand Binding Domain (AR-LBD)	nr_ar_lbd	Inactive	0.97
10.	Tox21-Nuclear receptor signalling pathways	Aromatase	nr_aromatase	Inactive	0.91
11.	Tox21-Nuclear receptor signalling pathways	Peroxisome Proliferator Activated Receptor Gamma (PPAR-Gamma)	nr_ppar_gamma	Inactive	0.99
12.	Tox21-Stress response pathways	Nuclear factor (erythroid-derived 2)-like 2/antioxidant responsive element (nrf2/ARE)	sr_are	Inactive	0.92
13.	Tox21-Stress response pathways	Heat shock factor response element (HSE)	sr_hse	Inactive	0.92
14.	Tox21-Stress response pathways	Phosphoprotein (Tumor Supressor) p53	sr_p53	Inactive	0.93
15.	Tox21-Stress response pathways	ATPase family AAA domain-containing protein 5 (ATAD5)	sr_atad5	Inactive	0.96
16.	Molecular Initiating Events	Thyroid hormone receptor alpha (THRα)	mie_thr_alpha	Inactive	0.90
17.	Molecular Initiating Events	Thyroid hormone receptor beta (THRβ)	mie_thr_beta	Inactive	0.99
18.	Molecular Initiating Events	Ryanodine receptor (RYR)	mie_ryr	Inactive	0.90
19.	Molecular Initiating Events	GABA receptor (GABAR)	mie_gabar	Inactive	0.55
20.	Molecular Initiating Events	Glutamate N-methyl-D-aspartate receptor (NMDAR)	mie_nmdar	Inactive	0.96
21.	Molecular Initiating Events	alpha-amino-3-hydroxy-5-methyl-4-isoxazolepropionate receptor (AMPAR)	mie_ampar	Inactive	1
22.	Molecular Initiating Events	Kainate receptor (KAR)	mie_kar	Inactive	1
23.	Molecular Initiating Events	Constitutive androstane receptor (CAR)	mie_car	Inactive	0.99
24.	Molecular Initiating Events	Pregnane X receptor (PXR)	mie_pxr	Inactive	0.55
25.	Molecular Initiating Events	NADH-quinone oxidoreductase (NADHOX)	mie_nadhox	Inactive	0.87
26.	Molecular Initiating Events	Voltage gated sodium channel (VGSC)	mie_vgsc	Inactive	0.95
27.	Molecular Initiating Events	Na+/I- symporter (NIS)	mie_nis	Inactive	0.91
28.	Metabolism	Cytochrome CYP2D6	CYP2D6	Inactive	0.86
29.	Metabolism	Cytochrome CYP3A4	CYP3A4	Inactive	0.85
30.	Metabolism	Cytochrome CYP2E1	CYP2E1	Inactive	0.99

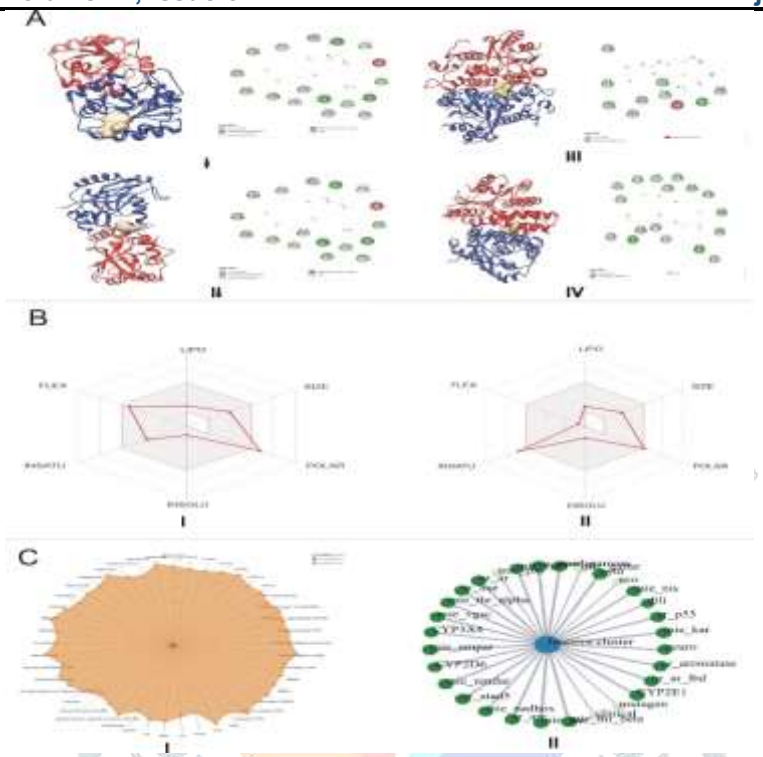

Fig1: (A) Molecular docking interaction between Valacyclovir and 1AT3 (I), Leucocianidol and 1AT3 (II), Valacyclovir and 1KI3 (III), Leucocianidol and 1KI3 (IV), **(B)** ADME radar view of Valacyclovir **(I)** and Leucocianidol **(II), (C)** Toxicity analysis of Leucocianidol radar view **(I),** network view **(II).**

DFT Analysis

DFT analysis of leucocianidol and valacyclovir, free and complexed with 1AT3 and 1KI3, revealed electronic properties (Table 4). Leucocianidol's lower ionization potential and HOMO energy versus valacyclovir indicate higher reactivity, with slight energy shifts upon binding. Valacyclovir's larger HOMO-LUMO gap suggests greater stability. Parameters like hardness, softness, electronegativity, and electrophilicity support leucocianidol's stronger interaction with target proteins, reinforcing docking results and its therapeutic potential.

Table4: HOMO, LUMO, ΔE (HOMO-LUMO Gap), Hardness (η), Softness (S) Electronegativity (χ) Electrophilicity Index (ω) Chemical Potential (μ) Ionization Potential (IP) Electron Affinity (EA) of Leucocianidol, Leucocianidol_1AT3, Leucocianidol_1KI3, Valacyclovir, Valacyclovir_1AT3, Valacyclovir_1KI3

Molecule	HOMO	LUMO	ΔE (HOMO-LUMO Gap)	Hardness (η)	Softness (S)	Electronegativity (χ)	Electrophilicity Index (ω)	Chemical Potential (μ)	Ionization Potential (IP)	Electron Affinity (EA)
Leucocianidol	-8.98	-0.08	8.9	4.45	0.1124	4.53	2.3057	-4.53	8.98	0.08
Leucocianidol_1AT3	-9.092	-0.1	8.992	4.496	0.1112	4.596	2.3491	-4.596	9.092	0.1
Leucocianidol_1KI3	-9.024	-0.016	9.008	4.504	0.111	4.52	2.268	-4.52	9.024	0.016
Valacyclovir	-10.806	-3.429	7.377	3.6885	0.1356	7.1175	6.8671	-7.1175	10.806	3.429
Valacyclovir_1AT3	-10.987	-3.463	7.524	3.762	0.1329	7.225	6.9379	-7.225	10.987	3.463
Valacyclovir_1KI3	-10.858	-3.464	7.394	3.697	0.1352	7.161	6.9353	-7.161	10.858	3.464

Molecular Dynamics Simulation

RMSD

Root Mean Square Deviation (RMSD) analysis assessed the structural stability of Type II Protease (1AT3) and Thymidine Kinase (1KI3) complexes with Valacyclovir and Leucocianidol over 100 ns (Fig 2 A, B). The 1AT3 apo form showed dynamic RMSD fluctuations (0.2–0.4 nm), while Valacyclovir and Leucocianidol complexes exhibited lower fluctuations, indicating enhanced stability. The 1AT3-Leucocianidol complex had the lowest RMSD (<0.3 nm), suggesting superior stabilization. Ligand RMSD for both compounds in 1KI3 remained stable (~0.3 nm), with Leucocianidol showing initial adjustments before stabilizing. These results highlight Leucocianidol's strong binding and stability, supporting its potential for further study.

RMSF

Root Mean Square Fluctuation (RMSF) analysis evaluated residue flexibility in Type II Protease (1AT3) and Thymidine Kinase (1KI3) complexes with Valacyclovir and Leucocianidol (Fig 2 C, D). The 1AT3 apo form showed high fluctuations (>0.6 nm) in loop regions, reduced upon ligand binding. The 1AT3-Leucocianidol complex exhibited the lowest RMSF values, indicating enhanced rigidity compared to Valacyclovir. For 1KI3, both ligands decreased apo form fluctuations (>0.5 nm), though

Leucocianidol showed slightly higher flexibility in some residues. These results, consistent with RMSD findings, highlight Leucocianidol's superior stabilization of 1AT3, supporting its potential as a strong binding candidate.

Radius of Gyration

Radius of Gyration (Rg) analysis assessed the compactness of Type II Protease (1AT3) and Thymidine Kinase (1KI3) complexes with Valacyclovir and Leucocianidol over 100 ns (Fig 2 E, F). The 1AT3 apo form showed stable Rg (2.45–2.55 nm), with slight increases upon ligand binding, indicating minor expansion. The 1AT3-Leucocianidol complex had marginally higher Rg than 1AT3-Valacyclovir, suggesting localized flexibility. For 1KI3, apo Rg (2.45–2.50 nm) decreased slightly with ligands, with 1KI3-Leucocianidol showing the most compactness, enhancing rigidity. Both ligands maintain structural integrity, with Leucocianidol's compactness in 1KI3 supporting its inhibitory potential.

Radius of Gyration

Radius of Gyration (Rg) analysis assessed the compactness of Type II Protease (1AT3) and Thymidine Kinase (1KI3) complexes with Valacyclovir and Leucocianidol over 100 ns (Fig 2 G, H). The 1AT3 apo form showed stable Rg (2.45–2.55 nm), with slight increases upon ligand binding, indicating minor expansion. The 1AT3-Leucocianidol complex had marginally higher Rg than 1AT3-Valacyclovir, suggesting localized flexibility. For 1KI3, apo Rg (2.45–2.50 nm) decreased slightly with ligands, with 1KI3-Leucocianidol showing the most compactness, enhancing rigidity. Both ligands maintain structural integrity, with Leucocianidol's compactness in 1KI3 supporting its inhibitory potential.

SASA

Solvent-accessible surface area (SASA) analysis evaluated ligand-induced conformational changes in 1AT3 and 1KI3 over 100 ns (Fig 2 I, J). Apo 1AT3 SASA remained stable (~200 nm^2), with slight increases upon Valacyclovir and Leucocianidol binding, the latter showing higher values, suggesting dynamic interactions. Apo 1KI3 SASA stabilized at ~270 nm^2 after an initial rise, with Valacyclovir and Leucocianidol reducing SASA, indicating compactness, particularly with Leucocianidol. Leucocianidol's pronounced effect on 1AT3 (increased SASA) and 1KI3 (reduced SASA) compared to Valacyclovir supports its stronger binding potential, complementing H-bond findings.

PCA

Principal component analysis (PCA) examined conformational dynamics of 1AT3 and 1KI3 with Valacyclovir and Leucocianidol over 100 ns (Fig 2 K, L). Apo 1AT3 showed restricted conformational spread, while Valacyclovir increased flexibility, and Leucocianidol confined the distribution, indicating stabilization. For 1KI3, apo showed moderate spread, Valacyclovir enhanced dispersion, and Leucocianidol clustered tightly, suggesting rigidity. Valacyclovir increases flexibility in both proteins, while Leucocianidol restricts conformational space, supporting its stabilizing effect and inhibitory potential, consistent with RMSD and SASA findings.

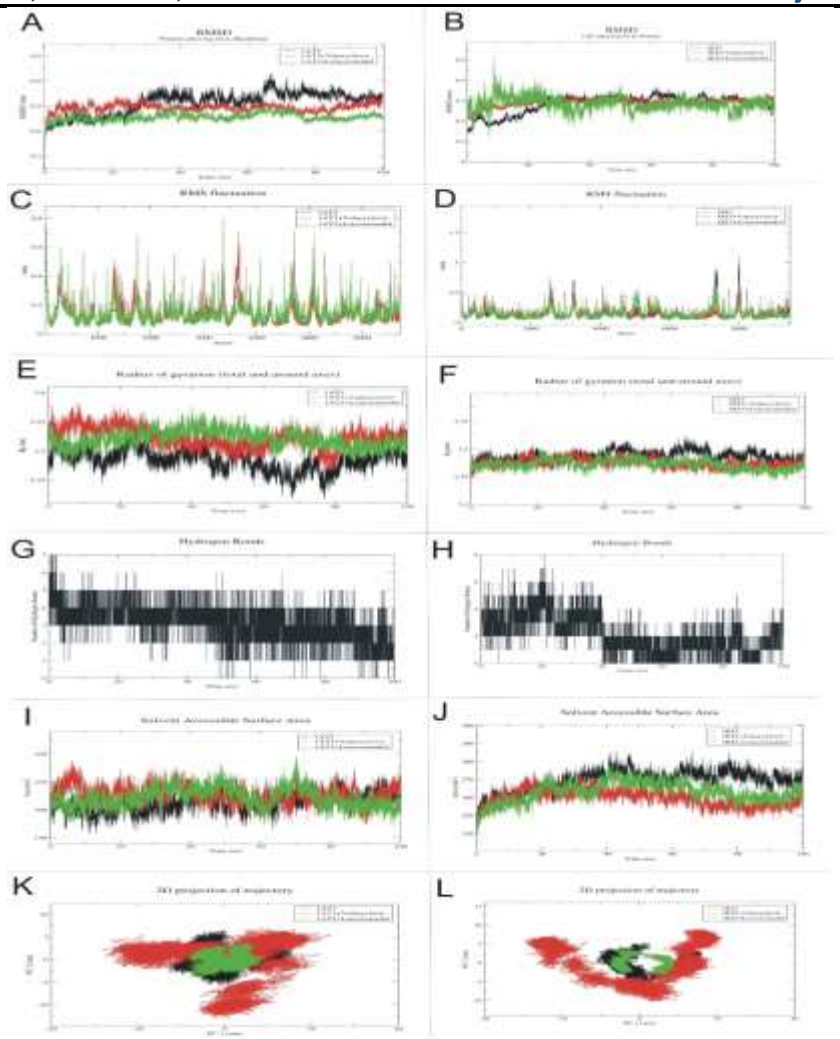

Fig 2. MD Simulation analysis of Valacyclovir and Leucocianidol with IAT3 and 1KI3: RMSD (A & B), RMSF (C & D), Rg (E & F), H-Bond (G & H), SASA (I & J), PCA (K & L)

FEL

Free Energy Landscape (FEL) analysis assessed conformational stability of 1AT3 and 1KI3 with Valacyclovir and Leucocianidol using PC1 and PC2 (Fig3 a-f). Apo 1AT3 showed multiple shallow energy basins, indicating flexibility, while Leucocianidol binding formed a deep, stable minimum, unlike Valacyclovir's broader, less stable distribution. Similarly, apo 1KI3 displayed metastable states, with Leucocianidol inducing a localized energy minimum and Valacyclovir increasing fluctuations. Leucocianidol stabilizes both proteins' conformations, contrasting Valacyclovir's dynamic effects, aligning with PCA and RMSD findings and supporting its superior inhibitory potential.

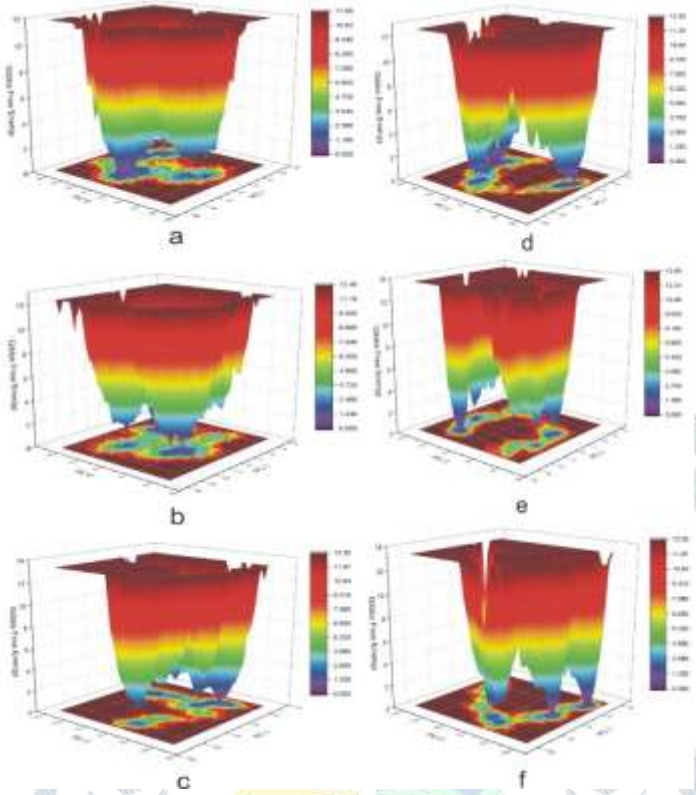

Fig 3: FEL, analysis of 1AT3 (a), 1AT3+ Leucocianidol (b), 1AT3+ Valacyclovir (c), and 1KI3 (d), 1KI3+ Leucocianidol (e), 1KI3+ Valacyclovir (f)

Conclusion

This study demonstrates that Leucocianidol is a promising antiviral candidate against herpes virus thymidine kinase (1AT3) and type II protease (1KI3), exhibiting superior binding affinity and stability compared to Valacyclovir. Through molecular docking, MD simulations, PCA, and FEL analysis, Leucocianidol consistently stabilized protein-ligand complexes, reducing conformational flexibility and forming deeper energy minima. Its favorable ADMET profile supports its potential as a drug-like molecule with high bioavailability and low toxicity. While these in-silico findings are robust, in future experimental validation via enzymatic assays, in vitro, and in vivo studies are essential to confirm biological efficacy and explore Leucocianidol's effects on other viral targets, employ advanced sampling techniques, and develop optimized derivatives to enhance its therapeutic potential against herpes virus infections.

Statements and Declarations

Acknowledgments.

The authors sincerely express their gratitude to **Singhania University** for providing the necessary support and research facilities to conduct this study.

Conflict of interest.

The authors declare that there is no conflict of interest regarding the publication of this research.

Author contributions.

Shivam Mishra conducted all the research work, including analysis, interpretation, and manuscript preparation. Prabhat Kumar and Nidhi Mishra, supervised the entire study, providing guidance and critical insights throughout the research process.

References

[1] Abraham, M. J., Murtola, T., Schulz, R., Páll, S., Smith, J. C., Hess, B., & Lindahl, E. (2015). GROMACS: High performance molecular simulations through multi-level parallelism from laptops to supercomputers. *SoftwareX, 1-2*, 19–25. https://doi.org/10.1016/j.softx.2015.06.001

[2] Amadei, A., Linssen, A. B. M., & Berendsen, H. J. C. (1993). Essential dynamics of proteins. *Proteins: Structure, Function, and Bioinformatics, 17*(4), 412–425. https://doi.org/10.1002/prot.340170407

[3] Armaković, S., Armaković, S. J., & Abramović, B. F. (2016). Theoretical investigation of loratadine reactivity in order to understand its degradation properties: DFT and MD study. *Journal of molecular modeling*, *22*, 1-14. DOI: 10.1007/s00894-016-3101-2

[4] Baker, E. N., & Hubbard, R. E. (1984). Hydrogen bonding in globular proteins. *Progress in Biophysics and Molecular Biology, 44*(2), 97–179. https://doi.org/10.1016/0079-6107(84)90007-5

[5] Banerjee, P., Eckert, A. O., Schrey, A. K., & Preissner, R. (2018). ProTox-II: A webserver for the prediction of toxicity of chemicals. *Nucleic Acids Research, 46*(W1), W257–W263. https://doi.org/10.1093/nar/gky318

[6] Bayly, C. I., Cieplak, P., Cornell, W. D., & Kollman, P. A. (1993). A well-behaved electrostatic potential based method using charge restraints for deriving atomic charges: The RESP model. *The Journal of Physical Chemistry, 97*(40), 10269–10280. https://doi.org/10.1021/j100142a004

[7] Berendsen, H. J. C., Postma, J. P. M., van Gunsteren, W. F., DiNola, A., & Haak, J. R. (1984). Molecular dynamics with coupling to an external bath. *The Journal of Chemical Physics, 81*(8), 3684–3690. https://doi.org/10.1063/1.448118

[8] Champness, J. N., Bennett, M. S., Wien, F., Visse, R., Summers, W. C., Herdewijn, P., ... & Sanderson, M. R. (1998). Exploring the active site of herpes simplex virus type-1 thymidine kinase by X-ray crystallography of complexes with aciclovir and other ligands. *Proteins: Structure, Function, and Bioinformatics*, *32*(3), 350-361. DOI: 10.1002/(sici)1097-0134(19980815)32:3<350::aid-prot10>3.0.co;2-8

[9] Daina, A., Michielin, O., & Zoete, V. (2017). SwissADME: A free web tool to evaluate pharmacokinetics, drug-likeness, and medicinal chemistry friendliness of small molecules. *Scientific Reports, 7*, 42717. https://doi.org/10.1038/srep42717

[10] Das, D., & Hong, J. (2019). Herpesvirus polymerase inhibitors. In *Viral Polymerases* (pp. 333-356). Academic Press. https://doi.org/10.1016/B978-0-12-815422-9.00012-7

[11] Durand, D., Vivès, C., Cannella, D., Pérez, J., Pebay-Peyroula, E., Vachette, P., & Fieschi, F. (2010). NADPH oxidase activator p67phox behaves as a natively unfolded protein with folded protein–binding regions. *Journal of Biological Chemistry, 285*(10), 6318–6326. https://doi.org/10.1074/jbc.M109.063230

[12] Gibbs, J. W. (1878). On the equilibrium of heterogeneous substances. *Transactions of the Connecticut Academy of Arts and Sciences, 3*, 108–248.

[13] Hanson, R. M. (2010). Jmol—A paradigm shift in scientific visualization. *Journal of Cheminformatics, 2*, 1. https://doi.org/10.1186/1758-2946-2-1.

[14] Hanwell, M. D., Curtis, D. E., Lonie, D. C., Vandermeersch, T., Zurek, E., & Hutchison, G. R. (2012). Avogadro: An advanced semantic chemical editor, visualization, and analysis platform. *Journal of Cheminformatics, 4*, 17. https://doi.org/10.1186/1758-2946-4-17

[16] Hoog, S. S., Smith, W. W., Qiu, X., Janson, C. A., Hellmig, B., McQueney, M. S., ... & Abdel-Meguid, S. S. (1997). Active site cavity of herpesvirus proteases revealed by the crystal structure of herpes simplex virus protease/inhibitor complex. *Biochemistry*, *36*(46), 14023-14029. DOI: 10.1021/bi9712697

[17] Jorgensen, W. L., Chandrasekhar, J., Madura, J. D., Impey, R. W., & Klein, M. L. (1983). Comparison of simple potential functions for simulating liquid water. *The Journal of Chemical Physics, 79*(2), 926–935. https://doi.org/10.1063/1.445869.

[18] Kabsch, W., & Sander, C. (1983). Dictionary of protein secondary structure: Pattern recognition of hydrogen-bonded and geometrical features. *Biopolymers, 22*(12), 2577–2637. https://doi.org/10.1002/bip.360221211

[19] Kumari, I., Kaurav, H., & Chaudhary, G. (2021). Phytomedicinal value of Saraca asoca (ashoka) in enhancing female reproductive systemin ayurveda and folk system of medicine. *Int J Pharmacognosy*, *8*(6), 193-03. DOI: 10.18520/v109/i10/1790-1801

[20] Lautenschlager, S. (2020). Human herpes viruses. *Braun-Falco´s Dermatology*, 1-24. DOI: 10.1007/978-3-662-58713-3_9-1

[21] Lee, B., & Richards, F. M. (1971). The interpretation of protein structures: Estimation of static accessibility. *Journal of Molecular Biology, 55*(3), 379–400. https://doi.org/10.1016/0022-2836(71)90324-X

[22] Levitt, M. (1983). Molecular dynamics of native protein: I. Computer simulation of trajectories. *Journal of Molecular Biology, 168*(3), 595–617. https://doi.org/10.1016/S0022-2836(83)80325-5

[23] Ma, Y., Frutos-Beltrán, E., Kang, D., Pannecouque, C., De Clercq, E., Menéndez-Arias, L., ... & Zhan, P. (2021). Medicinal chemistry strategies for discovering antivirals effective against drug-resistant viruses. *Chemical Society Reviews*, *50*(7), 4514-4540. DOI: **https://doi.org/10.1039/D0CS01084G**

[24] Maltarollo, V. G., Gertrudes, J. C., Oliveira, P. R., & Honorio, K. M. (2015). Applying machine learning techniques for ADME-Tox prediction: a review. *Expert opinion on drug metabolism & toxicology*, *11*(2), 259-271. DOI: 10.1517/17425255.2015.980814

[25] McLachlan, A. D. (1982). A mathematical procedure for superimposing atomic coordinates of proteins. *Acta Crystallographica Section A: Foundations of Crystallography, 38*(6), 871–873. https://doi.org/10.1107/S0567739482001735

[26] Mettenleiter, T. C., Ehlers, B., Müller, T., Yoon, K. J., & Teifke, J. P. (2019). Herpesviruses. *Diseases of swine*, 548-575. **https://doi.org/10.1002/9781119350927.ch35**

[27] Mishra, S., Modanwal, S., Kumar, P., Mishra, A., & Mishra, N. (2025). Computational Evaluation of Punica granatum Leaf Phytochemicals against Multi-drug Resistant E. coli: Molecular Docking, ADMET, MD Simulation, and DFT Studies. *Current Computer-Aided Drug Design*. http://dx.doi.org/10.2174/0115734099343126241105102839.

[28] Morris, G. M., Huey, R., Lindstrom, W., Sanner, M. F., Belew, R. K., Goodsell, D. S., & Olson, A. J. (2009). AutoDock4 and AutoDockTools4: Automated docking with selective receptor flexibility. *Journal of Computational Chemistry, 30*(16), 2785–2791. https://doi.org/10.1002/jcc.21256

[29] Panigrahi, D., & Sahu, S. K. (2025). Computational approaches: atom-based 3D-QSAR, molecular docking, ADME-Tox, MD simulation and DFT to find novel multi-targeted anti-tubercular agents. *BMC chemistry*, *19*(1), 39. DOI:https://doi.org/10.1186/s13065-024-01357-2

[30] Parrinello, M., & Rahman, A. (1981). Polymorphic transitions in single crystals: A new molecular dynamics method. *Journal of Applied Physics, 52*(12), 7182–7190. https://doi.org/10.1063/1.328693

[31] Qader, S. W., Suvitha, A., Ozdemir, M., Benjamin, I., Nsa, A. S. R., Akem, M. U., ... & Eluwa, E. C. (2022). Investigating the physicochemical properties and pharmacokinetics of curcumin employing density functional theory and gastric protection. *Chemical Physics Impact*, *5*, 100130. DOI: doi:10.1016/j.chphi.2022.100130

[32] Rao, F., & Caflisch, A. (2004). The protein folding free energy surface: A survey of minimalist lattice models. *Journal of Chemical Physics, 119*(1), 240–250. https://doi.org/10.1063/1.1577332

[33] Rathod, C. P., & Ghante, M. H. (2021). Pharmacological importance of Saraca asoca: a review. *Research journal of pharmacognosy and phytochemistry*, *13*(3), 131-135. 10.52711/0975-4385.2021.00022

[34] Sharma, A., & Gupta, S. P. (2017). Fundamentals of viruses and their proteases. In *Viral proteases and their inhibitors* (pp. 1-24). Academic Press. https://doi.org/10.1016/B978-0-12-809712-0.00001-0

[35] Stewart, J. J. P. (2016). MOPAC2016. *Stewart Computational Chemistry.* http://openmopac.net

[36] Treml, J., Gazdová, M., Šmejkal, K., Šudomová, M., Kubatka, P., & Hassan, S. T. (2020). Natural products-derived chemicals: Breaking barriers to novel anti-HSV drug development. *Viruses*, *12*(2), 154. DOI: 10.3390/v12020154

[37] Trott, O., & Olson, A. J. (2010). AutoDock Vina: Improving the speed and accuracy of docking with a new scoring function, efficient optimization, and multithreading. *Journal of Computational Chemistry, 31*(2), 455–461. https://doi.org/10.1002/jcc.21334

[38] Vanommeslaeghe, K., Hatcher, E., Acharya, C., Kundu, S., Zhong, S., Shim, J., Darian, E., Guvench, O., Lopes, P., Vorobyov, I., & MacKerell, A. D., Jr. (2010). CHARMM general force field: A force field for drug-like molecules compatible with the CHARMM all-atom additive biological force fields. *Journal of Computational Chemistry, 31*(4), 671–690. https://doi.org/10.1002/jcc.21367

[39] Vivek-Ananth, R. P., Mohanraj, K., Sahoo, A. K., & Samal, A. (2023). IMPPAT 2.0: an enhanced and expanded phytochemical atlas of Indian medicinal plants. *ACS omega*, *8*(9), 8827-8845. DOI: https://doi.org/10.1021/acsomega.3c00156

[40] Xie, Y., Wu, L., Wang, M., Cheng, A., Yang, Q., Wu, Y., ... & Chen, X. (2019). Alpha-herpesvirus thymidine kinase genes mediate viral virulence and are potential therapeutic targets. *Frontiers in microbiology*, *10*, 941. https://doi.org/10.3389/fmicb.2019.00941